Damage-Based Design Earthquake Loads for Single-Degree-Of-Freedom Inelastic Structures

Abbas Moustafa[1]

Abstract: This paper develops a new framework for modeling design earthquake loads for inelastic structures. Limited information on strong ground motions is assumed to be available only at the given site. The design earthquake acceleration is expressed as a Fourier series, with unknown amplitude and phase angle, modulated by an envelope function. The design ground acceleration is estimated by solving an inverse dynamic problem, using nonlinear programming techniques, so that the structure performance is minimized. At the same time, the design earthquake is constrained to the available information on past recorded ground motions. New measures of the structure performance based on energy concepts and damage indexes are introduced in this paper. Specifically, the structural performance is quantified in terms of Park and Ang damage indexes. Damage indexes imply that the structure is damaged by a combination of repeated stress reversals and high-stress excursions. Furthermore, the use of damage indexes provides a measure on the structure damage level, and making a decision on necessary repair possible. The material stress-strain relationship is modeled as either bilinear or elastic-plastic. The formulation is demonstrated by deriving the design earthquake loads for inelastic frame structures at a firm soil site. The damage spectra for the site are also established, to provide upper bounds of damage under possible future earthquakes. **DOI: 10.1061/(ASCE)ST.1943-541X.0000074.**

CE Database subject headings: Ductility; Damage; Optimization; Earthquake loads; Seismic design; Inelasticity; Earthquake resistant structures.

Author keywords: Design earthquake loads; Input energy; Inelastic structures; Ductility ratio; Hysteretic energy; Damage indexes; Damage spectra; Nonlinear optimization.

Introduction

The assessment of seismic performance of structures under future earthquakes is an important problem in earthquake engineering. The basic objective of the structural engineer is to design structures that are safe against possible future earthquakes and economical at the same time. To achieve this goal, the following criteria should be fulfilled: (1) robust definition of earthquake ground motions for the site, (2) accurate mathematical model for the material behavior, and (3) reliable structural damage descriptors that accurately describe possible structural damage under seismic loads.

The earthquake-resistant design of structures has been an active area of research for many decades. Early works have dealt with specifying earthquake loads in terms of the elastic and inelastic design response spectra for the site (e.g., Mahin and Bertero 1981; Newmark and Hall 1982; Riddell 1995), specifying the time history of the ground acceleration (e.g., Bommer and Acevedo 2004), or using the theory of random vibrations (e.g., Kiureghian and Crempien 1989; Conte and Peng 1997). Hazard response spectra have also been established by many researchers (e.g., Reiter 1990 and McGuire 1995). The development of mathematical models to describe the hysteretic nonlinear behavior of the structure during earthquakes has been carried out by several researchers (e.g., Takeda et al. 1970; Otani 1981; Akiyama 1985). However, the inadequate performance of structures during recent earthquakes has motivated researchers to revise existing methods and to develop new methods for seismic-resistant design. This includes new design concepts, such as, energy-based design (e.g., Akiyama 1985; Goel 1997; Decanini and Mollaiodi 2001; Wong and Yang 2002), performance-based design (e.g., Park et al. 1985; Fajfar 1992; Fajfar and Krawinkler 1997; SEAOC 2000; Bozorgnia and Bertero 2004; Choi and Kim 2006) and optimum damper placement for seismic-resistant design (e.g., Nakashima et al. 1996; Yamaguchi and El-Abd 2003).

This paper develops a new framework for specifying robust design earthquake loads for seismic-resistant design of structures using the method of critical excitations. This method relies on the high uncertainty associated with the occurrence of earthquakes and their characteristics (e.g., time, location, magnitude, duration, frequency content, and amplitude), and also on the safety requirements of important and lifeline structures (e.g., nuclear plants, storage tanks, and industrial installations). A limited material on modeling critical earthquakes for nonlinear structures is available in the literature (e.g., Moustafa 2002; Abbas 2006; Takewaki 2002, 2007). Drenick and Iyengar provided early research thoughts on this subject. Iyengar (1972) computed critical seismic inputs for nonlinear Duffing oscillators by constraining the input energy. Drenick (1977) derived critical excitations for nonlinear systems in terms of the impulse response of the linearized system. Philippacopoulos and Wang (1984) expressed the critical input as a linear summation of recorded accelerograms and established critical inelastic response spectra for the site. This series representation, however, is questionable. Westermo (1985) used calculus of

[1]Department of Civil Engineering, School of Engineering, Nagasaki Univ., Nagasaki 852-8521, Japan, and Dept. of Civil Engineering, Faculty of Engineering, Minia Univ., Minia 61111, Egypt (corresponding author). E-mail: abbas.moustafa@eng.miniauniv.edu.eg; abbas.moustafa@yahoo.com

Note. This manuscript was submitted on June 23, 2008; approved on March 30, 2009; published online on February 15, 2011. Discussion period open until August 1, 2011; separate discussions must be submitted for individual papers. This paper is part of the ***Journal of Structural Engineering***, Vol. 137, No. 3, March 1, 2011. ©ASCE, ISSN 0733-9445/2011/3-456–467/$25.00.

variation to show that the critical inputs for elastic-plastic systems are not harmonic. Recently, Takewaki (2001) used the equivalent linearization method to estimate critical probabilistic earthquakes for elastic-plastic structures that maximize the interstory drift. Abbas (2006) derived critical seismic loads for inelastic structures by maximizing the ductility ratio. Similarly, probabilistic critical earthquakes were computed for inelastic and parametrically excited structures by using first-order reliability method (FORM) and response surface approximations (Sarkar 2003; Abbas and Manohar 2005, 2007).

From the above discussion it can be seen that most of the aforementioned research work is either conceptual, uses approximations in representing the ground motion or in calculating the structure response or is based on maximization of single response parameter. This paper avoids these approximations and introduces modern measures of structural damage to develop robust earthquake loads on inelastic structures. The structure performance is quantified using Park and Ang damage indexes and thus a quantitative measure of the structure damage and necessary repair are possible.

Response and Damage Characterization of Inelastic Structures under Earthquake Loads

This section demonstrates briefly the seismic-response analysis and energy quantification for single-degree-of-freedom (SDOF) inelastic structures under earthquake loads. Subsequently, the use of inelastic response parameters and energy absorbed by the structure in developing damage indexes is explained.

Dynamic Analysis of Inelastic Structures

The equation of motion for a nonlinear SDOF structure under a single component of earthquake acceleration $\ddot{x}_g(t)$ is given as

$$m\ddot{x}(t) + c\dot{x}(t) + f_s(t) = -m\ddot{x}_g(t) \tag{1}$$

where m and c = mass and damping coefficient of the structure, respectively; $f_s(t)$ = spring hysteretic restoring force; $x(t)$ = structure displacement and dot indicates differentiation with respect to time. Fig. 1 depicts the relationship between the inelastic deformation and the spring hysteretic force for bilinear and elastic-plastic materials. Eq. (1) can be rewritten as

$$\ddot{x} + 2\eta_0\omega_0\dot{x} + \omega_0^2 x_y \bar{f}_s(t) = -\ddot{x}_g(t) \tag{2}$$

Here η_0 and ω_0 = preyield damping ratio and natural frequency; x_y = yield displacement; and $\bar{f}_s(t)$ = normalized hysteretic force. Eq. (2) can be further recast as

$$\ddot{\mu}(t) + 2\eta_0\omega_0\dot{\mu}(t) + \omega_0^2\bar{f}_s(t) = -\omega_0^2\frac{\ddot{x}_g(t)}{a_y} \tag{3}$$

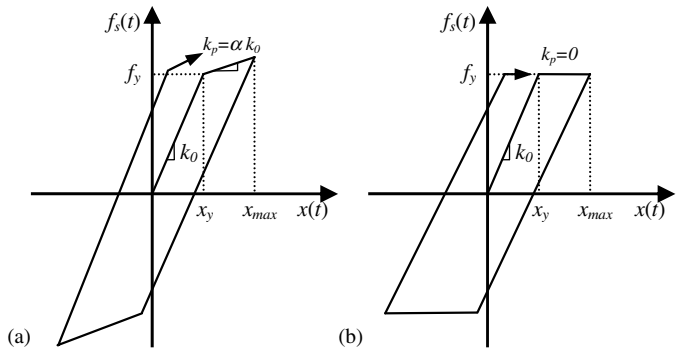

Fig. 1. Force-displacement relation for nonlinear materials: (a) bilinear model; (b) elastic-plastic model

where $\mu(t) = x(t)/x_y$ = ductility ratio; and $a_y = f_y/m$ = constant that can be interpreted as the acceleration of the mass necessary to produce the yield force. The response of inelastic SDOF structures can be computed by solving the incremental form of Eqs. (1) and (3) using numerical integration at discrete points of time. In this study, we use the Newmark β-method. For bilinear behavior, an iterative procedure is adopted to correct for approximations of the secant stiffness used from previous time step. The next subsection demonstrates the quantification of the earthquake input energy and associated energy dissipated by the structure.

Earthquake Input Energy and Energy Dissipated by Inelastic Structures

The energy balance for the SDOF inelastic structure can be obtained by multiplying Eq. (1) by the relative velocity $\dot{x}(\tau)$ and integrating, thus (Zahrah and Hall 1984; Akiyama 1985; Uang and Bertero 1990; Takewaki 2004; Kalkan and Kunnath 2008)

$$\int_0^t m\ddot{x}(\tau)\dot{x}(\tau)d\tau + \int_0^t c\dot{x}^2(\tau)d\tau + \int_0^t f_s(\tau)\dot{x}(\tau)d\tau = -\int_0^t m\ddot{x}_g(\tau)\dot{x}(\tau)d\tau \tag{4a}$$

$$E_K(t) + E_D(t) + E_S(t) = E_I(t) \tag{4b}$$

Eqs. (4*a*) and (4*b*) represent the relative energy terms (see, e.g., Uang and Bertero 1990; Kalkan and Kunnath 2008). Here $E_I(t)$ is the earthquake relative input energy to the structure, because the ground shakes until it comes to rest. $E_K(t)$ is the relative kinetic energy $[E_K(t) = m\dot{x}^2(t)/2]$ and $E_D(t)$ is the energy absorbed by damping. The energy $E_S(t)$ represents the total relative energy absorbed by the spring and is composed of the recoverable elastic energy and the hysteretic cumulative plastic energy $E_H(t)$.

At the end of the earthquake duration the kinetic and elastic strain energies diminish. Thus, the earthquake input energy to the structure is dissipated by the hysteretic and the damping energies. The next section demonstrates the use of the response parameters and plastic energy in developing damage indexes.

Safety Assessment of Inelastic Structures Using Damage Indexes

The literature on damage measures of structures under ground motions is vast (e.g., Cosenza et al. 1993; Ghobarah et al. 1999). Damage indexes are based on either a single or combination of structural response parameters. Table 1 summarizes several damage measures that are based on a single response parameter (Powell and Allahabadi 1988; Cosenza et al. 1993). The first measure indicates the ultimate ductility produced during the ground shaking. Clearly, this measure does not incorporate any information on how the earthquake input energy is imparted on the structure nor how this energy is dissipated. Earthquake damage occurs not only due to the maximum deformation or ductility but is associated with the hysteretic energy dissipated by the structure as well. The definition of structural damage, in terms of the ductility factor, is inadequate. The last three measures indicate the rate of the earthquake input energy to the structure (i.e., how fast E_I is imparted by the earthquake and how fast it gets dissipated). Damage indexes can be estimated by comparing the response parameters demanded by the earthquake with the structural capacities. Powell and Allahabadi (1988) proposed a damage index in terms of the ultimate ductility (capacity)μ_u and the maximum ductility attained during ground shaking $\mu_{\max}$:

Table 1. Response Descriptors for Inelastic Buildings under Earthquake Ground Motion

S. no.	Response parameter	Definition
1	Maximum ductility	$\mu_{\max} = \max_{0\le t\le t_f}\lvert x(t)/x_y\rvert$
2	Number of yield reversals	Number of times velocity changes sign
3	Maximum normalized plastic deformation range	$\Delta\bar{x}_{p,i} = \max_{0\le t\le t_f}\lvert\Delta x_{p,i}/x_y\rvert$
4	Normalized cumulative ductility	$\mu_{\text{ac.}} = \sum_{i=1}^{N}\lvert\Delta x_{p,i}\rvert/x_y + 1$
5	Residual (permanent) ductility	$\mu_{\text{res}} = \lvert x(t_f)/x_y\rvert$
6	Normalized earthquake input energy	$\bar{E}_I = 1/(f_y x_y)\int_0^{t_f} E_I(t)dt$
7	Normalized total hysteretic energy dissipated	$\bar{E}_H = 1/(f_y x_y)\int_0^{t_f} E_H(t)dt$
8	Ratio of total hysteretic energy to input energy	$r_E = \bar{E}_H/\bar{E}_I$
9	Maximum rate of normalized input energy	$P_{I,\max} = \max_{0\le t\le t_f}[dE_I(t)/dt]/(f_y x_y)$
10	Maximum rate of normalized damping energy	$P_{D,\max} = \max_{0\le t\le t_f}[dE_D(t)/dt]/(f_y x_y)$
11	Maximum rate of normalized hysteretic energy	$P_{H,\max} = \max_{0\le t\le t_f}[dE_H(t)/dt]/(f_y x_y)$

$$DI_\mu = \frac{x_{\max} - x_y}{x_u - x_y} = \frac{\mu_{\max} - 1}{\mu_u - 1} \tag{5}$$

However, DI_μ does not include effects from hysteretic energy dissipation. Cosenza et al. (1993) and Fajfar (1992) proposed a damage index based on the structure hysteretic energy E_H:

$$DI_H = \frac{E_H/(f_y x_y)}{\mu_u - 1} \tag{6}$$

A robust damage measure should include not only the maximum response but the effect of repeated cyclic loading as well. Park and coworkers developed a simple damage index, given as (Park et al. 1985; Park and Ang 1985; Park et al. 1987)

$$DI_{PA} = \frac{x_{\max}}{x_u} + \beta\frac{E_H}{f_y x_u} = \frac{\mu_{\max}}{\mu_u} + \beta\frac{E_H}{f_y x_y \mu_u} \tag{7}$$

Here $x_{\max}$ and E_H = maximum displacement and dissipated hysteretic energy (excluding elastic energy) under the earthquake. Note that $x_{\max}$ is the maximum absolute value of the displacement response under ground motion, x_u is the ultimate deformation capacity under monotonic loading and β is a positive constant that weights the effect of cyclic loading on structural damage. If $\beta = 0$, the contribution to DI_{PA} from cyclic loading is omitted.

The state of the structure damage is defined as: (a) repairable damage, when $DI_{PA} < 0.40$, (b) damaged beyond repair, when $0.40 \le DI_{PA} < 1.0$, and (c) total or complete collapse, when $DI_{PA} \ge 1.0$. These criteria are based on calibration of DI_{PA} against experimental results and field observations in earthquakes (Park et al. 1987). The Park and Ang damage index reveals that both maximum ductility and hysteretic energy dissipation contribute to the structure resistance during ground motions. In Eq. (7) damage is expressed as a linear combination of the damage caused by excessive deformation and that contributed by repeated cyclic loading effect. Also, the quantities $x_{\max}$, E_H depend on the loading history while the quantities β, x_u, f_y are independent of the loading history and are determined from experimental tests. In this paper we adopt Park and Ang damage index in deriving the design earthquakes. The next section develops this formulation.

Damage-Based Design Earthquake Loads for Inelastic Structures

The derivation of critical earthquake loads for SDOF inelastic structures is developed in this section. The ground acceleration is represented as a product of a Fourier series and an envelope function:

$$\ddot{x}_g(t) = e(t)\sum_{i=1}^{N_f} R_i\cos(\omega_i t - \varphi_i) = A_0[\exp(-\alpha_1 t) - \exp(-\alpha_2 t)]\sum_{i=1}^{N_f} R_i\cos(\omega_i t - \varphi_i) \tag{8}$$

Here A_0 = scaling constant, and the parameters α_1, α_2 impart the transient nature to $\ddot{x}_g(t)$. Next, R_i and φ_i are $2N_f$ unknown amplitudes and phase angles, respectively and ω_i, $i = 1, 2, \ldots, N_f$ are the frequencies presented in the ground acceleration that are selected to span satisfactory the frequency range of $\ddot{x}_g(t)$. In constructing critical seismic inputs, the envelope function is taken to be fully known. The information on energy E, peak ground acceleration (PGA) M_1, peak ground velocity (PGV) M_2, peak ground displacement (PGD) M_3, upper bound Fourier amplitude spectra (UBFAS) $M_4(\omega)$, and lower bound Fourier amplitude spectra (LBFAS) $M_5(\omega)$ are also taken to be available, which enables defining the following constraints (Abbas and Manohar 2002; Abbas 2006):

$$\left[\int_0^\infty \ddot{x}_g^2(t)dt\right]^{1/2} \le E \qquad \max_{0<t<\infty}|\ddot{x}_g(t)| \le M_1$$
$$\max_{0<t<\infty}|\dot{x}_g(t)| \le M_2 \qquad \max_{0<t<\infty}|x_g(t)| \le M_3$$
$$M_5(\omega) \le |X_g(\omega)| \le M_4(\omega) \tag{9}$$

Here $X_g(\omega)$ = Fourier transform of $\ddot{x}_g(t)$. The constraint on the earthquake energy is related to the Arias intensity (Arias 1970). The UBFAS and LBFAS constraints aim to replicate the frequency content and amplitude observed in past recorded accelerograms on the design earthquake. The ground velocity and displacement are obtained from Eq. (8) as follows:

$$\dot{x}_g(t) = \sum_{i=1}^{N_f}\int_0^t R_i e(\tau)\cos(\omega_i\tau - \varphi_i)d\tau + C_1;$$
$$x_g(t) = \sum_{i=1}^{N_f}\int_0^t R_i e(\tau)(t-\tau)\cos(\omega_i\tau - \varphi_i)d\tau + C_1 t + C_2 \tag{10}$$

Making use of the conditions $x_g(0) = 0$ and $\lim_{t\to\infty}\dot{x}_g(t) \to 0$ (Shinozuka and Henry 1965), the constants in the above Eq. can be shown to be given as (Abbas and Manohar 2002; Abbas 2006):

$$C_2 = 0; \qquad C_1 = -\sum_{i=1}^{N_f}\int_0^\infty R_i e(\tau)\cos(\omega_i\tau - \varphi_i)d\tau \tag{11}$$

The constraints of Eq. (9) can be expressed in terms of the variables R_i, φ_i, $i = 1, 2, \ldots, N_f$ as

$$\left[A_0^2\sum_{m=1}^{N_f}\sum_{n=1}^{N_f}R_mR_n\int_0^\infty[\exp(-\alpha_1 t)-\exp(-\alpha_2 t)]^2\cos(\omega_m t-\varphi_m)\cos(\omega_n t-\varphi_n)dt\right]^{1/2}\le E$$

$$\max_{0<t<\infty}\left|A_0[\exp(-\alpha_1 t)-\exp(-\alpha_2 t)]\sum_{n=1}^{N_f}R_n\cos(\omega_n t-\varphi_n)\right|\le M_1$$

$$\max_{0<t<\infty}\left|A_0\sum_{n=1}^{N_f}\int_0^t R_n[\exp(-\alpha_1\tau)-\exp(-\alpha_2\tau)]\cos(\omega_n\tau-\varphi_n)d\tau-A_0\sum_{n=1}^{N_f}\int_0^\infty R_n[\exp(-\alpha_1\tau)-\exp(-\alpha_2\tau)]\cos(\omega_n\tau-\varphi_n)d\tau\right|\le M_2$$

$$\max_{0<t<\infty}\left|A_0\sum_{n=1}^{N_f}\int_0^t R_n[\exp(-\alpha_1\tau)-\exp(-\alpha_2\tau)](t-\tau)\cos(\omega_n\tau-\varphi_n)d\tau\right.$$
$$\left.-A_0 t\sum_{n=1}^{N_f}\int_0^\infty R_n[\exp(-\alpha_1\tau)-\exp(-\alpha_2\tau)]\cos(\omega_n\tau-\varphi_n)d\tau\right|\le M_3$$

$$M_5(\omega)\le\left|A_0\sum_{n=1}^{N_f}\int_0^\infty R_n\{\exp[-\alpha_1\tau]-\exp[-\alpha_2\tau]\}\cos(\omega_n\tau-\varphi_n)\exp[-i\omega\tau]d\tau\right|\le M_4(\omega) \quad (12)$$

Here $i=\sqrt{-1}$. To quantify the constraints quantities E, M_1, M_2, M_3, $M_4(\omega)$, and $M_5(\omega)$ it is assumed that a set of N_r earthquake records denoted by $\ddot{v}_{gi}(t)$, $i=1,2,\ldots,N_r$ are available for the site under consideration or from other sites with similar geological soil conditions. The values of energy, PGA, PGV and PGD are obtained for each of these records. The highest of these values across all records define E, M_1, M_2, and M_3. The available records are further normalized such that the Arias intensity of each record is set to unity (i.e.,$[\int_0^\infty \ddot{v}_{gi}^2(t)dt]^{1/2}=1$, Arias 1970), and are denoted by $\{\bar{\ddot{v}}_{gi}\}_{i=1}^{N_r}$. The bounds $M_4(\omega)$ and $M_5(\omega)$ are obtained as

$$M_4(\omega)=E\max_{1\le i\le N_r}|\bar{V}_{gi}(\omega)|;\qquad M_5(\omega)=E\min_{1\le i\le N_r}|\bar{V}_{gi}(\omega)| \quad (13)$$

Here $\bar{V}_{gi}(\omega)$, $i=1,2,\ldots,N_r$ denotes the Fourier transform of the ith normalized accelerogram $\bar{\ddot{v}}_{gi}(t)$. The bound $M_4(\omega)$ has been considered earlier (Shinozuka 1970; Takewaki 2001; 2002). The lower bound was considered by Moustafa (2002) and Abbas and Manohar (2002).

Finally, the problem of deriving critical earthquake loads for inelastic structures can be posed as determining the optimization variables $y=\{R_1,R_2,\ldots,R_{N_f},\varphi_1,\varphi_2,\varphi_3\ldots,\varphi_{N_f}\}^t$ such that DI_{PA} is maximized subjected to the constraints of Eq. (12). The solution to this nonlinear constrained optimization problem is tackled by using the sequential quadratic programming method (Arora 2004). The following convergence criteria are adopted:

$$|f_j-f_{j-1}|\le\varepsilon_1;\qquad |y_{i,j}-y_{i,j-1}|\le\varepsilon_2 \quad (14)$$

Here f_j = objective function at the jth iteration; $y_{i,j}$ = ith optimization variable at the jth iteration; and ε_1, ε_2 = small quantities to be specified. The structure inelastic deformation is estimated using the Newmark β-method which is built as a subroutine inside the optimization program. The details of the procedure involved in the computation of the optimal earthquake and the associated damage index are shown in Fig. 2.

The quantities $\mu(t)$ and $E_H(t)$ do not reach their respective maxima at the same time. Therefore, the optimization is performed at discrete points of time and the optimal solution $y^*=[R_1^*,R_2^*,\ldots,R_{N_f}^*,\varphi_1^*,\varphi_2^*,\ldots,\varphi_{N_f}^*]^t$ is the one that produces the maximum DI_{PA} across all time points. The critical earthquake loads are characterized in terms of the critical accelerations and associated damage indexes, inelastic deformations and energy dissipated by the structure. The next section provides numerical illustrations for the formulation developed in this section.

In the numerical analysis, the constraints quantities E, M_1, M_2, M_3, $M_4(\omega)$, and $M_5(\omega)$ are estimated using past recorded earthquake data. These quantities are taken as the extreme values of the associated parameters across the set of past recorded ground motions. These parameters define the energy, PGA, PGV, PGD, and upper and lower bounds on the Fourier amplitude spectra of past recorded ground motions at the site under consideration or other sites with similar geological soil conditions. This approach is considered to be consistent with the aspirations of the ground-motion models that are commonly used by engineers, that basically aim to replicate some of the gross features of recorded motions, such as amplitude, frequency content, nonstationarity trend, local soil amplification effects, and duration. Predictive or physical models for ground motions that take into account several details, such as fault dimension, fault orientation, rupture velocity, magnitude of earthquake, attenuation, stress drop, density of the intervening medium, local soil condition, and epicentral distance, have also been developed in the existing literature, mainly by seismologists (see, e.g., Brune 1970; Hanks and McGuire 1981; Boore 1983; Queck et al. 1990). In using these models, one needs to input values for a host of parameters and the success of the model depends upon how realistically this is done. It is possible to formulate the optimal earthquake models based on the latter class of models where one can aim to optimize the parameters of the model to realize the least favorable conditions. It is important to consider that the class of admissible functions, in the determination of critical excitations, in this case, becomes further constrained by the choice that one makes for the physical model. The approach adopted in this study, in this sense, is nonparametric in nature. A comparison of results based on this approach with those from "model-based" approaches is of interest; however, these questions are not considered in the present study.

Numerical Illustrations and Discussions

Bilinear Inelastic Frame Structure

We consider a SDOF building frame with mass 9×10^3 kg, initial stiffness $k_0=1.49\times10^5$ N/m and viscous damping of 0.03 damping ratio. The initial natural frequency was computed as 4.07 rad/s

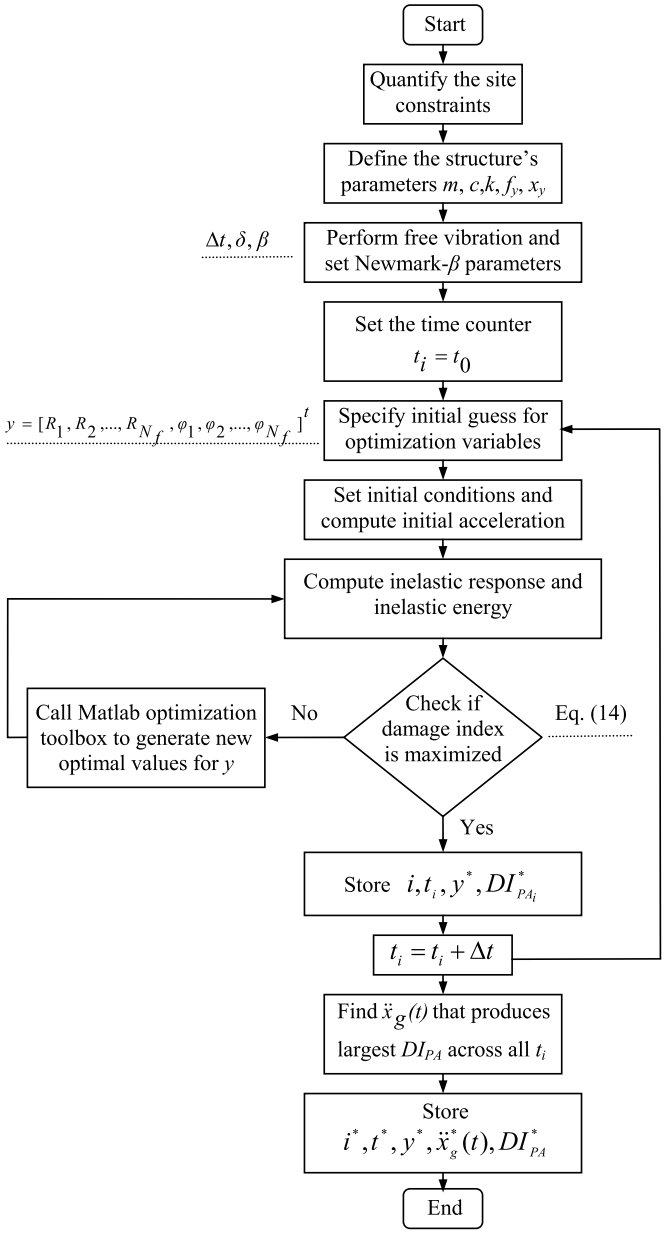

Fig. 2. Flowchart for deriving optimal earthquake loads

and the strain hardening ratio is taken as 0.05. These parameters are changed later to study their influence on the estimated optimal earthquake loads and corresponding inelastic deformations. The yield displacement is taken as 0.10 m and the structure is taken to start from rest. The objective function is adopted as the Park and Ang damage index DI_{PA} given by Eq. (7). The parameters of the Newmark β-method are taken as $\delta = 1/2$; $\alpha = 1/6$; and $\Delta t = 0.005$ s.

Earthquake Data at the Site and Quantification of Constraints

A set of 20 earthquake ground motions is used to quantify the constraint bounds E, M_1, M_2, M_3, $M_4(\omega)$, and $M_5(\omega)$ [Consortium of Organizations for Strong Motion Observation Systems (COSMOS) 2005]. Table 2 provides information on these records (Abbas 2006). Based on numerical analyses of these records the constraints were computed as $E = 4.17$ m/s$^{1.5}$, $M_1 = 4.63$ m/s^2 (0.47 g), $M_2 = 0.60$ m/s and $M_3 = 0.15$ m. The average dominant frequency of the ground accelerations was about 1.65 Hz. The envelope parameters were taken as $A_0 = 2.17$, $\alpha_1 = 0.13$, and $\alpha_2 = 0.50$. The convergence limits ε_1, ε_2 were taken as 10^{-6} and the convergence criterion on the secant stiffness is taken as 10^{-3} N/m.

The frequency content for $\ddot{x}_g(t)$ is taken as (0.1–25) Hz. Additionally, in distributing the frequencies ω_i, $i = 1, 2, \ldots, N_f$ in the interval (0.1,25), it was found advantageous to select some of these ω_i to coincide with the natural frequency of the elastic structure, and also to place relatively more points within the modal half-power bandwidth.

The constraint scenarios considered in deriving the optimal earthquake inputs are listed in Table 3. The constrained nonlinear optimization problem is tackled using the sequential quadratic optimization algorithm "fmincon" of the Matlab optimization toolbox (Caleman et al. 1999). In the numerical calculations, alternative initial starting solutions, within the feasible region, were examined and were found to lead to the same optimal solution. To select the number of frequency terms N_f a parametric study was carried out and $N_f = 51$ was found to give satisfactory results. Fig. 3 depicts the influence of the frequency terms N_f on the convergence of the objective function for constraints scenarios 1 and 4 (see Table 3).

Results and Discussions

The numerical results obtained are presented in Figs. 4–9 and Table 4. Fig. 4 shows results for constraint scenario 1 and similar results for case 4 are shown in Fig. 5. Each of these figures shows the Fourier amplitude spectrum of the optimal ground acceleration, the inelastic deformation, the hysteretic force and the energy dissipated by the structure. Fig. 6 shows the time history of the ground acceleration and velocity for cases 1 and 4. Based on extensive analyses of the numerical results, the following observations are made:

1. The frequency content and Fourier amplitude of the design earthquake are strongly dependent on the constraints imposed (see Table 3). If available information on earthquake data is limited to the total energy and PGA, the design input is narrow band (highly resonant) and the structure deformation is conservative (see Fig. 4 and Table 4). Furthermore, most of the power of the Fourier amplitude is concentrated at a frequency close to the natural frequency of the elastic structure. This amplitude gets shifted away from the natural frequency toward a higher frequency when the strain hardening ratio increases. The Fourier amplitudes at other frequencies are low and uniformly distributed. The results of this constraint scenario match well with earlier work reported by this writer for elastic-plastic structures (Abbas 2006) and also by Takewaki (2001) on probabilistic earthquake inputs for elastic-plastic structures. This result, however, is substantially different from that for the elastic structure where all power of the acceleration amplitude is concentrated around ω_0 with no amplitude at other frequencies (Abbas and Manohar 2002). Additional constraints on the Fourier amplitude spectra (see Table 3) force the Fourier amplitude of the optimal acceleration to get distributed across other frequencies. The critical acceleration possesses a dominant frequency that is close to the average dominant frequency observed in past records (see Fig. 5). The realism of the earthquake input is also evident from the maximum damage index it produces. For instance, the damage index for case 4 is 0.37 which is substantially smaller than 1.15 for case 1 (Table 4). The constraints on PGV and PGD were not found to be significant in producing realistic critical inputs compared to the constraints on UBFAS and LBFAS. Also, the realism of the

Table 2. Information on Past Ground-Motion Records for Firm Soil Site

Earthquake date	Magnitude	Epic. dist. (km)	Component	PGA (m/s^2)	PGV (m/s)	PGD (m)	Energy[a] ($m/s^{1.5}$)	Site
Mamoth Lakes	6.2	1.5	W	4.02	0.21	0.05	3.73	Convict Greek
05.25.1980			S	3.92	0.23	0.05	4.01	
Loma Prieta	7.0	9.7	W	3.91	0.31	0.07	3.82	Capitola
10.18.1989			S	4.63	0.36	0.11	2.61	
Morgan Hill	6.1	4.5	S60E	3.06	0.40	0.07	2.33	Halls Valley
04.24.1984			S30W	1.53	0.30	0.02	1.64	
San Fernando	6.6	27.6	N69W	3.09	0.17	0.04	2.07	Castaic Old Ridge
02.09.1971			N21E	2.66	0.28	0.10	2.47	
Parkfield	5.0	9.1	W	2.88	0.44	0.01	1.33	Parkfield fault
12.20.1994			S	3.80	0.10	0.01	1.74	
Caolinga	6.5	30.1	W	2.83	0.26	0.10	2.67	Cantua Creek
05.02.1983			N	2.20	0.26	0.10	2.14	
Northridge	6.7	5.9	S74E	3.81	0.60	0.12	4.17	Canoga Park
01.17.1994			S16W	3.43	0.34	0.09	3.50	
Cape Mendocino	7.0	5.4	W	3.25	0.45	0.15	2.44	Petrolia general
04.25.1992			S	2.89	0.24	0.08	2.31	
Westmorland	5.0	6.6	E	4.35	0.33	0.11	3.26	Westmorland fire
04.26.1981			S	3.54	0.44	0.15	3.25	
Imperial Valley	6.4	17.4	S45W	2.68	0.22	0.10	2.30	Calexico fire
10.15.1979			N45W	1.98	0.19	0.15	2.14	

[a] $E = [\int_0^\infty \ddot{v}_g^2(t)dt]^{1/2}$ (Arias 1970).

Table 3. Nomenclature of Constraint Scenarios Considered

Case	Constraints imposed
1	Energy and PGA
2	Energy, PGA, PGV, and PGD
3	Energy, PGA, and UBFAS
4	Energy, PGA, UBFAS, and LBFAS

optimal acceleration for case 4 can be examined by comparing the Fourier amplitude spectra and frequency content of the design acceleration (Figs. 4 and 5) with the Fourier amplitude spectra of past recorded earthquakes (Fig. 7). It may be emphasized that while the constraint scenario 1 leads to pulselike ground motion, such scenario was in deed observed during some of the recent earthquakes (e.g., 1971 San Fernando, 1985 Mexico, and 1995 Hyogoken-Nanbu earthquakes). Resonant or pulselike earthquakes are also observable in near-field ground motion with directivity focusing, known as forward- and backward-directivity ground motion, which resemble fault-parallel and fault-normal components (Housner and Hudson 1958; Kalkan and Kunnath 2006; He and Agrawal 2008; Moustafa 2008). The realism of optimal earthquake loads can be also examined by comparing maximum response from optimal accelerations with those from past recorded ground motions. Thus, the maximum ductility factor of the structure from the design earthquake is about 3.9 (case 1) and 2.6 (case 4) times that from the Hyogoken-Nanbu earthquake and is 2.7 (case 1) and 1.5 (case 4) times that from the San Fernando earthquake.

2. To examine the effect of the strain hardening ratio on the design earthquake acceleration computed, limited studies were carried out. The value of α was changed and the critical input was determined by solving a new optimization problem. Namely, α was taken as 0.20, 0.10, 0.05, and 0.01. The strain hardening ratio was not seen to significantly influence the

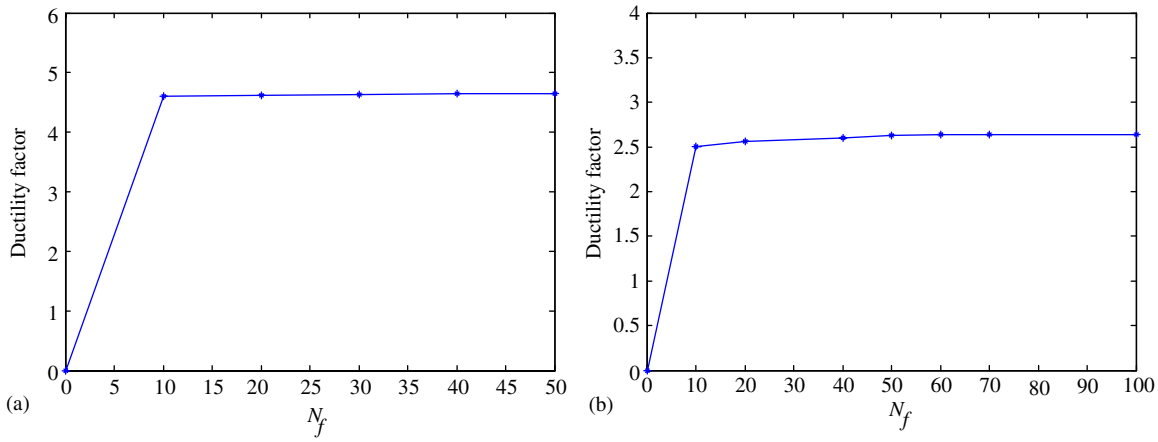

Fig. 3. Convergence of objective function in terms of frequency terms N_f: (a) Case 1; (b) Case 4

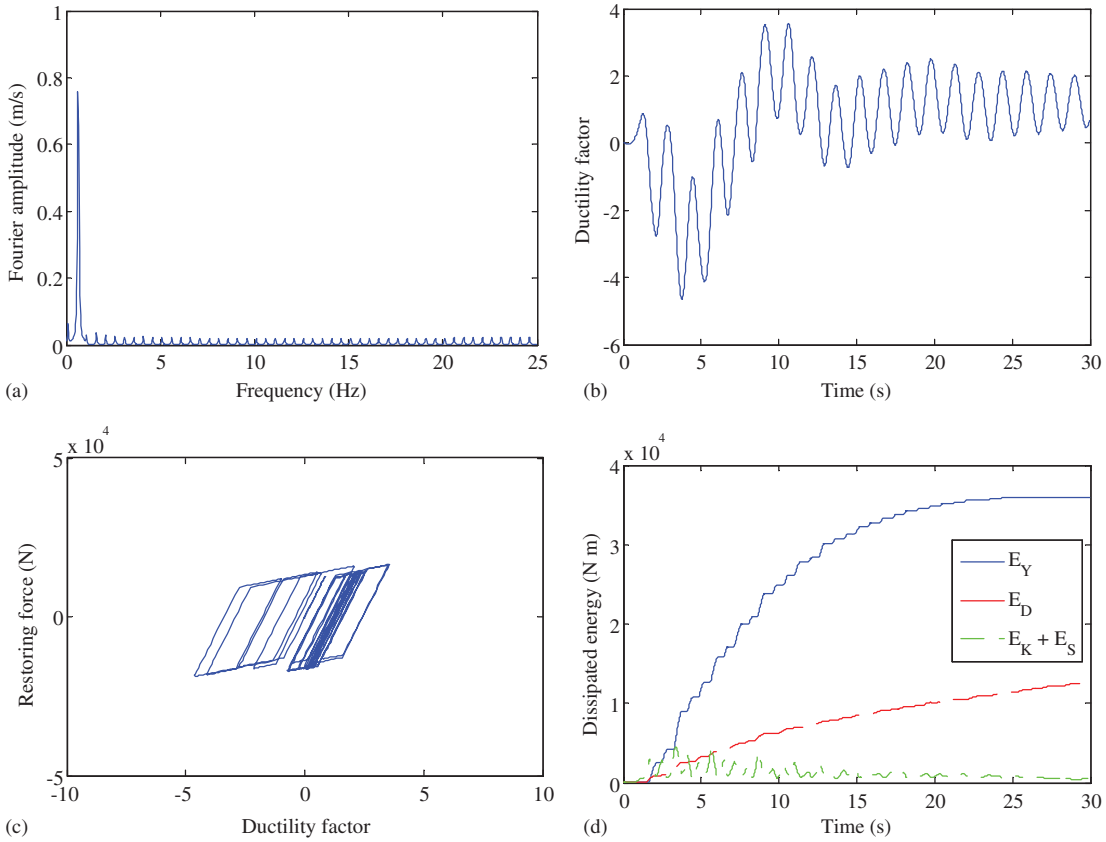

Fig. 4. Optimal earthquake input and associated structural responses for case 1: (a) Fourier amplitude of the ground acceleration; (b) inelastic deformation; (c) hysteretic restoring force; (d) dissipated energy

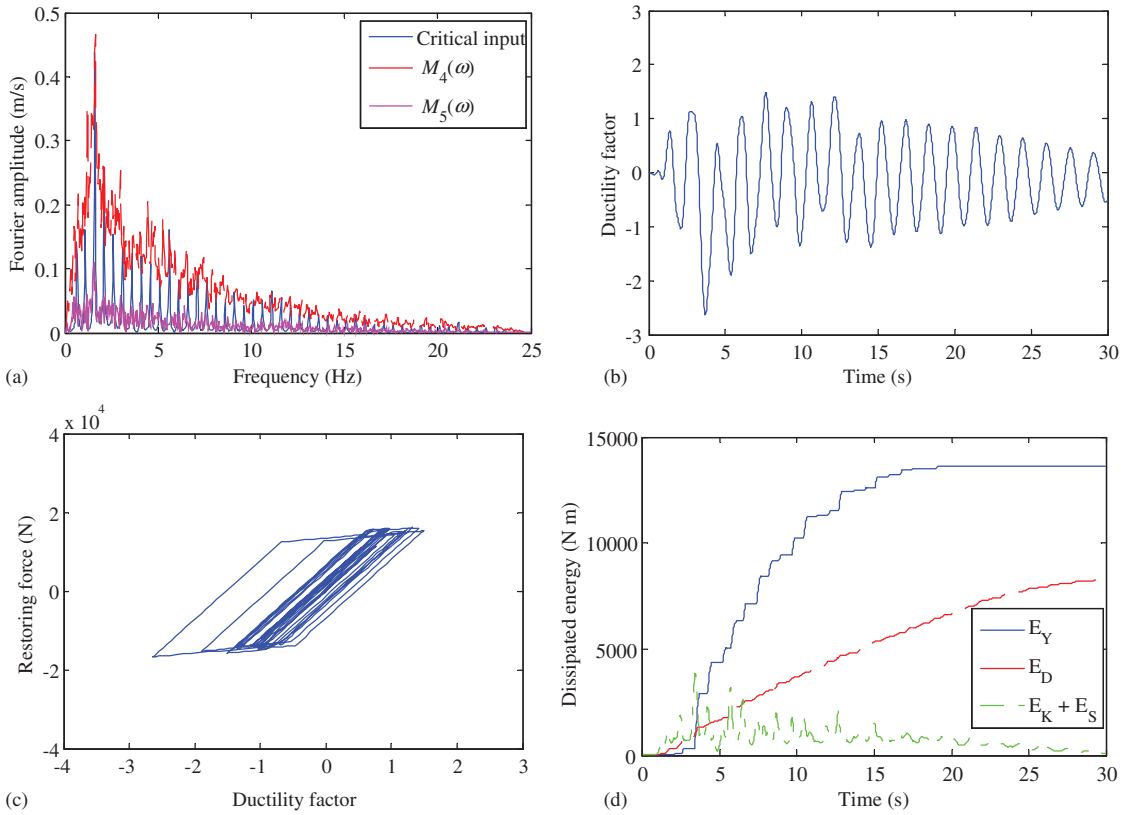

Fig. 5. Optimal earthquake input and associated structural responses for case 4: (a) Fourier amplitude of the ground acceleration; (b) inelastic deformation; (c) hysteretic restoring force; (d) dissipated energy

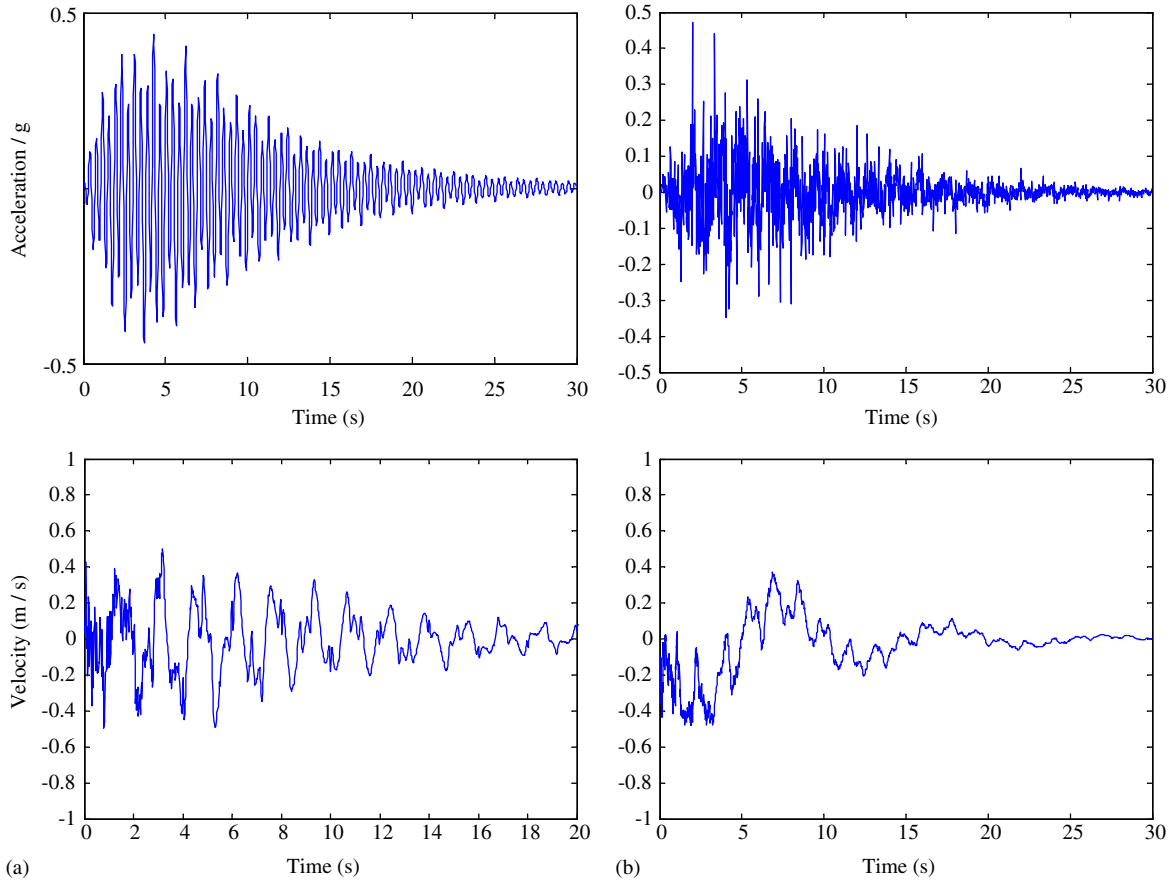

Fig. 6. Optimal earthquake acceleration and velocity: (a) Case 1; (b) Case 4

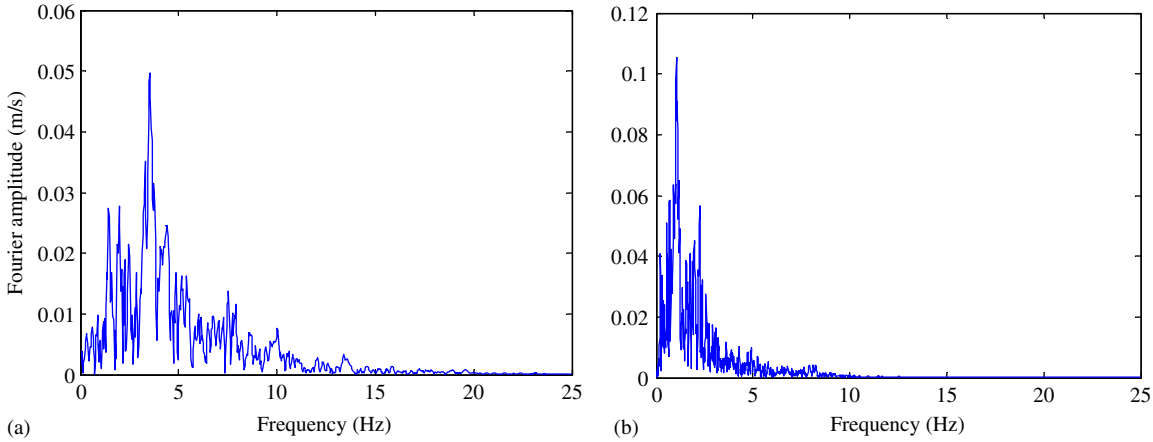

Fig. 7. Fourier spectra of recorded earthquakes: (a) San Fernando 1971; (b) Hyogoken-Nanbu 1995

frequency content of the critical earthquake input. It was observed, however, that the inelastic structure with lower values of α yields more frequently compared to the same structure with higher α values. Accordingly, the cumulative hysteretic energy dissipated was observed to decrease for higher values of α [Fig. 8(a)]. This feature is particularly remarkable at the end of the earthquake duration. It was also observed that the results on critical earthquake accelerations for bilinear inelastic structure with $\alpha = 0.01$ are close to those for the elastic-plastic structure (Abbas 2006).

3. To investigate the influence of the damping ratio on the computed design earthquake load, limited studies were carried out. The damping ratio was changed (namely, 0.01, 0.03, and 0.05) while all other parameters were kept unchanged. The critical earthquake is computed by solving a new optimization problem for each case. The effect of the change in η_0 was seen to be similar to that attributable to α. In other words, the value of the damping ratio was not seen to significantly influence the frequency content of the earthquake acceleration. It was observed, however, that the ductility ratio and the maximum inelastic deformation for the structure decrease for higher damping ratios. Thus, the ductility ratio decreases to 2.43 when the damping ratio is taken as 0.05 while the ductility ratio increases to 2.89 when the damping ratio reduces to 0.01.

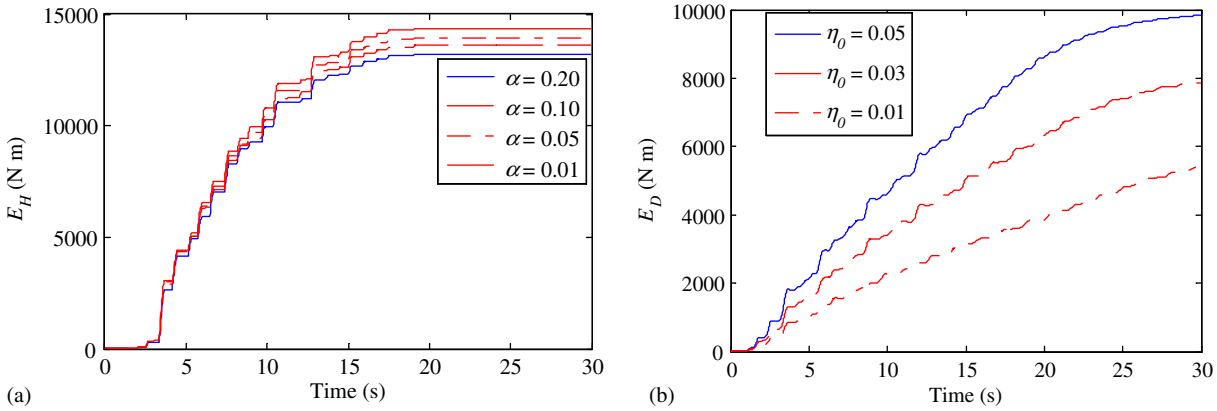

Fig. 8. (a) Effect of strain hardening ratio on dissipated yield energy; (b) effect of damping on dissipated damping energy

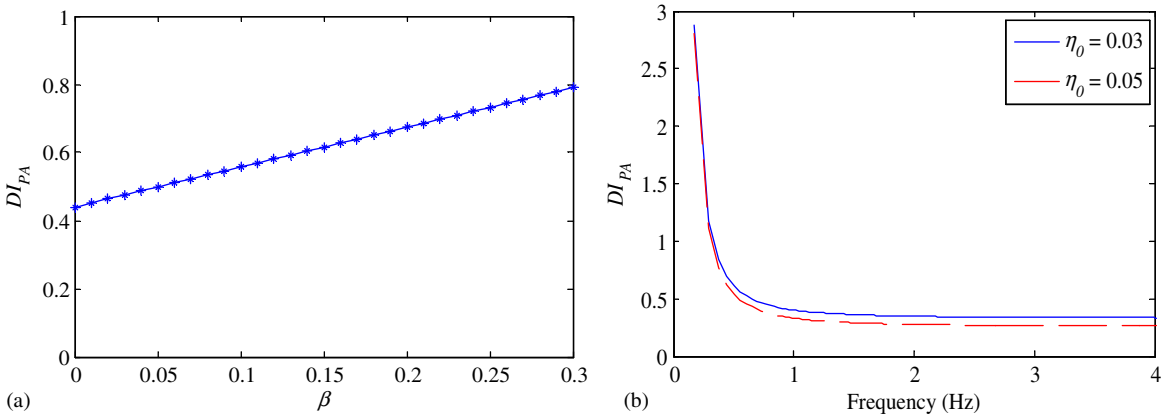

Fig. 9. (a) Effect of the value of β on the damage index; (b) damage spectra for SDOF inelastic structures

Table 4. Response Parameters for Alternative Constraint Scenarios ($\alpha = 0.05$, $\zeta = 0.03$)

Case	x_{max} (m)	μ_{max}	x_p (m)	N_{rv}[a]	DI_{PA}	Damage status
1	0.47	4.65	0.07	60	1.15	Total collapse
2	0.45	4.53	0.06	54	0.97	Damaged beyond repair
3	0.41	4.14	0.07	49	0.72	Damaged beyond repair
4	0.26	2.64	0.05	44	0.37	Repairable damage

[a]N_{rv} = number of yield reversals (see Table 1).

It was also observed that the inelastic structure with higher damping ratio dissipates more energy through damping compared with the same structure with lower damping ratio [see Fig. 8(b)]. The damage index also reduces when the damping ratio increases.

4. To assess the structure safety, Eq. (7) was used to estimate the damage index of the structure subjected to the critical earthquake load. We first examine the effect of the parameter β on the damage index. Based on experimental tests, it was reported that β ranges between 0.05 and 0.20 with an average value of 0.15 as suggested by Park et al. (1987). Fig. 9(a) shows the influence of β on the damage index. To study the effect of the initial natural frequency of the structure on the damage index, the structure stiffness was varied while keeping all other parameters unchanged and the critical earthquake was computed for each case. Subsequently, the value of DI_{PA} was calculated for each case. In the numerical calculations β was taken as 0.15 and x_{max}, μ_{max} are taken as 0.10 m and 2.64, respectively. The value of μ_u was taken as 6 in Fig. 9(a) and 8 in Fig. 9(b). It was found that the damage index for the structure with initial natural frequency smaller than 1.65 is higher than 0.40 and thus either total collapse or damage beyond repair of the structure is expected. The value of DI_{PA} for the structure with ω_0 greater than about 1.70 Hz is less than 0.40 and thus the structure does not experience total damage but repairable damage. This observation is consistent since the site dominant frequency is around 1.65 Hz and since the Fourier amplitude of the ground acceleration is seen to be located in the stiff side of the initial frequency of the inelastic structure.

The numeric illustrations of the formulation developed in this paper were demonstrated for simple structures modeled as

SDOF systems with bilinear and elastic-plastic force-deformation laws. The application of the proposed method to multi-degree-of-freedom (MDOF) structures and the use of more detailed degradation models (e.g., trilinear degradation, Takeda and Clough models) need to be investigated. Additionally, in this paper Park and Ang damage index has been used to assess the structure performance. This damage index has some limitations, which have been discussed by Mehanny and Deierlein (2000) and Bozorgenia and Bertero (2003). Among these drawbacks are: (1) its weak cumulative component for practical cases given the typical dominance of the peak displacement term over the accumulated energy term, (2) its format using a linear combination of deformation and energy in spite of the obvious nonlinearity of the problem and the interdependence of the two quantities, and (3) its lack of considering the loading sequence effect in the cumulative energy term. Furthermore, when $E_H = 0$ (elastic behavior), the value of DI_{PA} should be zero. However, the value of DI_{PA} computed from Eq. (7) will be greater than zero. Similarly, when the system reaches its maximum monotonic deformation, while DI_{PA} should be 1.0, however, Eq. (7) leads to DI_{PA} greater than 1.0. Chai et al. (1995) proposed modification to DI_{PA} to correct for the second drawback only. The study, also, examined experimentally the implication of the energy-based linear damage model of DI_{PA}. Despite the drawbacks of DI_{PA}, it has been extensively used by many researchers, mainly due to its simplicity and the extensive calibration against experimentally observed seismic structural damage during earthquakes (mainly for reinforced concrete structures). Bozorgenia and Bertero (2003) proposed two improved damage indexes that overcome some of the drawbacks associated with DI_{PA}.

In this paper, the optimal earthquakes that maximize the structural damage were obtained using deterministic methods. The design earthquake loads can be formulated based on hazard analysis using probability of occurrence, which provides a powerful alternative to the methodology developed in this paper.

Concluding Remarks

This paper developed a methodology for specifying earthquake ground motions as design inputs for inelastic structures at sites having limited earthquake data. New damage descriptors are introduced in deriving optimal earthquake loads. Specifically, the structural damage is quantified in terms of Park and Ang damage indexes. Damage indexes are mathematical models for quantitative description of the damage state of the structure and they correlate well with actual damage displayed during earthquakes. It is believed that the quantification of structural damage in terms of damage indexes is of substantial importance in deriving critical earthquake loads for inelastic structures. This is because damage indexes imply that the structure is damaged by a combination of repeated stress reversals and high-stress excursions. The quantification of the structure damage in terms of damage indexes makes it possible to assess the safety of the structure and provides an idea on necessary repair.

The design earthquake is estimated on the basis of available information using inverse dynamic analysis and nonlinear optimization methods. It was seen that if available information is limited to the energy and PGA, the resulting earthquake is highly resonant and produces conservative deformation. However, if extra information on the Fourier amplitude spectra is available, more realistic earthquakes are obtained, in terms of frequency content, amplitude, inelastic deformations and damage indexes they produce. The influences of the strain hardening and damping ratios on the estimated design loads were also studied. Critical damage spectra for the site were also established. These spectra provide an upper bound on structural damage and necessary repair under possible future earthquakes. The formulation developed in this paper was demonstrated for frame structures modeled as SDOF systems. The application of the proposed method to MDOF structures is currently under investigation. In this case, the global damage index of the structure is defined in terms of a weighted function of the damage indexes for the individual structural members.

Notation

The following symbols are used in this paper:

a_y = ratio of yield force to mass of the structure;
C_1, C_2 = quantities;
c = damping coefficient;
DI = damage index;
DI_{PA} = Ang and Park damage index;
E = Arias intensity (energy) of ground acceleration;
E_D = energy dissipated by damping;
E_H = hysteretic energy;
E_I = earthquake input relative energy;
E_k = kinetic energy;
E_S = strain energy
$e(t)$ = envelope function;
$f_s(t)$ = hysteretic restoring force;
f_y, x_y = yield force and yield displacement, respectively;
k_0, k_p = preyield and postyield stiffness;
M_1, M_2, M_3 = peak ground acceleration, velocity and displacement, respectively;
$M_4(\omega)$, $M_5(\omega)$ = lower and upper Fourier amplitude spectra, respectively;
m = mass;
N_f = number of frequencies;
R_i, φ_i = ith amplitude and phase angle of the ground acceleration;
t = time;
$\ddot{x}$, $\dot{x}$, x = acceleration, velocity and displacement responses of SDOF system, respectively;
$\ddot{x}_g$, $\dot{x}_g$, x_g = ground acceleration, velocity and displacement, respectively;
$x_{\max}$ = maximum displacement of inelastic structure;
x_u, μ_u = ultimate displacement and ductility under monotonic load;
A_0, α_1, α_2, β = positive quantities;
α = strain hardening ratio;
ε_1, ε_2 = small positive quantities;
η_0, ω_0 = damping ratio and natural frequency of elastic structure;
μ = ductility ratio; and
τ = dummy variable indicating time.

Acknowledgments

The author thanks three anonymous reviewers for their careful reading of the paper and insightful comments they made. This research work is partly supported by research funds from the Japanese Society for the Promotion of Science. The support is gratefully acknowledged.

References

Abbas, A. M. (2006). "Critical seismic load inputs for simple inelastic structures." *J. Sound Vib.*, 296, 949–967.

Abbas, A. M., and Manohar, C. S. (2002). "Investigations into critical earthquake load models within deterministic and probabilistic frameworks." *Earthquake Eng. Struct. Dyn.*, 31, 813–832.

Abbas, A. M., and Manohar, C. S. (2005). "Reliability-based critical earthquake load models, part 2: Nonlinear structures." *J. Sound Vib.*, 287, 883–900.

Abbas, A. M., and Manohar, C. S. (2007). "Reliability-based vector nonstationary random critical earthquake excitations for parametrically excited systems." *Struct. Saf.*, 29, 32–48.

Akiyama, H. (1985). *Earthquake-resistant limit-state design for buildings*, University of Tokyo Press, Tokyo.

Arias, A. (1970). *A measure of earthquake intensity: seismic design of nuclear power plants*, MIT Press, Cambridge, MA, 438–468.

Arora, J. S. (2004). *Introduction to optimum design*, Elsevier Academic, San Diego.

Bommer, J. J., and Acevedo, A. B. (2004). "The use of real earthquake accelerograms as input to dynamic analysis." *J. Earthquake Eng.*, 8, 43–91.

Boore, D. M. (1983). "Stochastic simulation of high-frequency ground motions based on seismological models of the radiated spectra." *Bull. Seismol. Soc. Am.*, 73(6a), 1865–94.

Bozorgenia, Y., and Bertero, V. V. (2003). "Damage spectra: Characteristics and applications to seismic risk reduction." *J. Struct. Eng.*, 129(10), 1330–1340.

Bozorgnia, Y., and Bertero, V. V., eds. (2004). *Earthquake engineering*, CRC Press, New York.

Brune, J. N. (1970). "Tectonic stress and the spectra of seismic shear waves from earthquakes." *J. Geophys. Res.*, 75, 4997–5009.

Caleman, T., Branch, M. A., and Grace, A. (1999). *Optimization toolbox for the use with Matlab: User's guide*, Math Works Inc., Natick, MA.

Chai, Y. H., Romstad, K. M., and Bird, S. M. (1995). "Energy-based linear damage model for high-intensity seismic loading." *J. Struct. Eng.*, 121(5), 857–864.

Choi, H., and Kim, J. (2006). "Energy-based design of buckling-restrained braced frames using hysteretic energy spectrum." *Eng. Struct.*, 28, 304–311.

Conte, J. P., and Peng, B. F. (1997). "Fully nonstationary analytical earthquake ground motion model." *J. Eng. Mech.*, 123, 15–24.

Cosenza, C., Manfredi, G., and Ramasco, R. (1993). "The use of damage functionals in earthquake engineering: a comparison between different methods." *Earthquake Eng. Struct. Dyn.*, 22, 855–868.

COSMOS. (2005). "Consortium organizations for strong-motion observation systems." ⟨http://db.cosmos-eq.org/scripts/default.plx⟩ (May 2008).

Decanini, L. D., and Mollaioli, F. (2001). "An energy-based methodology for the assessment of seismic demand." *Soil Dyn. Earthquake Eng.*, 21, 113–137.

Drenick, R. F. (1977). "The critical excitation of nonlinear systems." *J. Appl. Mech.*, 44(E2), 333–336.

Fajfar, P. (1992). "Equivalent ductility factors, taking into account low-cyclic fatigue." *Earthquake Eng. Struct. Dyn.*, 21, 837–848.

Fajfar, P., and Krawinklere, H., eds. (1997). *Seismic design methodologies for the next generation of codes*, Taylor & Francis, Rotterdam, Balkema.

Ghobara, A., Abou-Elfath, H., and Biddah, A. (1999). "Response-based damage assessment of structures." *Earthquake Eng. Struct. Dyn.*, 28, 79–104.

Goel, R. K. (1997). "Seismic response of asymmetric systems: energy-based approach." *J. Struct. Eng.*, 123(11), 1444–1453.

Hanks, T. G., and McGuire, R K. (1981). "The character of high frequency ground motions based on seismic shear waves." *Bull. Seismol. Soc. Am.*, 71(6), 2071–2095.

He, W.-L., and Agrawal, A. K. (2008). "Analytical model of ground motion pulses for the design and assessment of seismic protective systems." *J. Struct. Eng.*, 134(7), 1177–1188.

Housner, G. W., and Hudson, D. E. (1958). "The Port Hueneme earthquake of March 18, 1957." *Bull. Seismol. Soc. Am.*, 48, 163–168.

Iyengar, R. N. (1972). "Worst inputs and a bound on the highest peak statistics of a class of non-linear systems." *J. Sound Vib.*, 25, 29–37.

Kalkan, E., and Kunnath, S. K. (2006). "Effects of fling step and forward directivity on seismic response of buildings." *Earthquake Spectra*, 22(2), 367–390.

Kalkan, E., and Kunnath, S. K. (2008). "Relevance of absolute and relative energy content in seismic evaluation of structures." *Adv. Struct. Eng.*, 11(1), 1–18.

Kiureghian, A. D., and Crempien, J. (1989). "An evolutionary model for earthquake ground motion." *Struct. Saf.*, 6, 235–246.

Mahin, S. A., and Bertero, V. V. (1981). "An evaluation of inelastic seismic design spectra." *J. Struct. Div.*, 107(ST9), 1777–1795.

McGuire, R. K. (1995). "Probabilistic seismic hazard analysis and design earthquake: closing the loop." *Bull. Seismol. Soc. Am.*, 85(5), 1275–1284.

Mehanny, S. S., and Deierlein, G. G. (2000). "Modeling of assessment of seismic performance of composite frames with reinforced concrete columns and steel beams." *John Blume Earthquake Research Center Rep. No. 135*, Dept. of Civil and Environmental Engineering, Stanford Univ., Stanford, CA.

Moustafa, A. (2002). "Deterministic/Reliability-based critical earthquake load models for linear/nonlinear engineering structures," Ph.D. thesis, Dept. of Civil Engineering, Indian Institute of Science, Bangalore, India.

Moustafa, A. (2010). "Discussion of analytical model of ground motion pulses for the design and assessment of seismic protective systems." *J. Struct. Eng.*, 136(2), 229–230.

Nakashima, M., Saburi, K., and Tsuji, B. (1996). "Energy input and dissipation behavior of structures with hysteretic dampers." *Earthquake Eng. Struct. Dyn.*, 25, 483–496.

Newmark, N. M., and Hall, W. J. (1982). "Earthquake spectra and design, Monograph." Earthquake Engineering Research, Berkeley, CA.

Otani, S. (1981). "Hysteretic models of reinforced concrete for earthquake response analysis." *Journal of the Faculty of Engineering, University of Tokyo, Series B*, 36(2), 407–441.

Park, Y. J., and Ang, A. H.-S. (1985). "Mechanistic seismic damage model for reinforced concrete." *J. Struct. Eng.*, 111(4), 722–739.

Park, Y. J., Ang, A. H.-S., and Wen, Y. K. (1985). "Seismic damage analysis of reinforced concrete buildings." *J. Struct. Eng.*, 111(4), 740–757.

Park, Y. J., Ang, A. H.-S., and Wen, Y. K. (1987). "Damage-limiting aseismic design of buildings." *Earthquake Spectra*, 3(1), 1–26.

Philippacopoulos, A. J., and Wang, P. C. (1984). "Seismic inputs for nonlinear structures." *J. Eng. Mech.*, 110, 828–836.

Powell, G. H., and Allahabadi, R. (1988). "Seismic damage predictions by deterministic methods: concepts and procedures." *Earthquake Eng. Struct. Dyn.*, 16, 719–734.

Quek, S. T., Teo, Y. P., and Balendra, T. (1990). "Non-stationary structural response with evolutionary spectra using seismological input model." *Earthquake Eng. Struct. Dyn.*, 19, 275–288.

Reiter, L. (1990). *Earthquake hazard analysis*, Columbia University Press, New York.

Riddell, F. (1995). "Inelastic design spectra accounting for soil conditions." *Earthquake Eng. Struct. Dyn.*, 24, 1491–1510.

Sarkar, A. (2003). "Linear stochastic dynamical system under uncertain load: inverse reliability analysis." *J. Eng. Mech.*, 129(6), 665–671.

Shinozuka, M. (1970). "Maximum structural response to seismic excitations." *J. Eng. Mech. Div., Am. Soc. Civ. Eng.*, 96(5), 729–738.

Shinozuka, M., and Henry, L. (1965). "Random vibration of a beam column." *J. Eng. Mech. Div., Am. Soc. Civ. Eng.*, 91(5), 123–154.

Structural Engineers Association of California. (SEAOC), (2002). "Performance based seismic design engineering of buildings." *Vision 2000 Rep.*, Sacramento, CA.

Takeda, T., Sozen, M. A., and Nielsen, N.N. (1970). "Reinforced concrete response to simulated earthquakes." *J. Struct. Div.*, 96(ST12), 2557–2573.

Takewaki, I. (2001). "Probabilistic critical excitation for MDOF elastic-plastic structures on compliant ground." *Earthquake Eng. Struct. Dyn.*, 30, 1345–1360.
Takewaki, I. (2002). "Seismic critical excitation method for robust design: A review." *J. Struct. Eng.*, 128, 665–672.
Takewaki, I. (2004). "Bound of earthquake input energy." *J. Struct. Eng.*, 130, 1289–1297.
Takewaki, I. (2007). *Critical excitation methods in earthquake engineering*, Elsevier Science, The Netherlands.
Uang, C-M., Bertero, and V. V. (1990). "Evaluation of seismic energy in structures." *Earthquake Eng. Struct. Dyn.*, 19, 77–90.
Westermo, B. D. (1985). "The critical excitation and response of simple dynamic systems." *J. Sound Vib.*, 100, 233–242.
Wong, K. K. F., and Yong, R. (2002). "Earthquake response and energy evaluation of inelastic structures." *J. Eng. Mech.*, 128(3), 308–317.
Yamaguchi, H., and El-Abd, A. (2003). "Effect of energy input characteristics on hysteretic damper efficiency." *Earthquake Eng. Struct. Dyn.*, 32, 827–843.
Zahrah, T. F., and Hall, W. J. (1984). "Earthquake energy absorption in sdof structures." *J. Struct. Eng.*, 110, 1757–1772.